International Journal of Bifurcation and Chaos, Vol. 30, No. 9 (2020) 2030027 (21 pages)

DOI: 10.1142/S021812742030027X

Dynamics of Newton Maps of Quadratic Polynomial Maps of $\mathbb{R}^2$ into Itself

Roberto De Leo
Howard University,
Washington DC 20059, USA

Received November 16, 2019

We study numerically the α- and ω-limits of the Newton maps of quadratic polynomial transformations of the plane into itself. Our results confirm the conjectures posed in a recent work about the general dynamics of real Newton maps on the plane.

Keywords: Newton's method; Barna's theorem; discrete dynamical system; attractor; retractor; iterated function system.

1. Introduction

The dynamics of Newton maps of planar holomorphic maps has been extensively studied over the last hundred years as a chapter of the more general problem of the discrete dynamics of maps in one *complex* variable, after the seminal works of Julia [1918] and Fatou [1919, 1920a, 1920b]. This field saw a strong acceleration when computers became powerful enough to visualize the intricacies of their attractors and retractors, a moment often identified with the publication of the celebrated article of Mandelbrot on his homonymous fractal [Mandelbrot, 1980].

Despite the large number of articles and books dedicated to this topic and to its extension to general rational functions (we mention here just the classic books by Beardon [2000] and Milnor [2006] and the rich survey by Lyubich [1986] and refer the interested reader to [De Leo, 2019] for extensive comments and bibliography on this topic), very little attention has been dedicated so far, on the contrary, to Newton maps associated with *general* (as opposed to *holomorphic*) maps on the plane. There are indeed only a handful of articles dedicated to this topic: a series of articles by Peitgen and Richter [1986], Peitgen *et al.* [1988, 1989] in the late eighties where, in particular, they study some case relative to some of the simplest (but still far from trivial) polynomial maps in two variables, in particular quadratic ones; an article by Miller and Yorke [2000] where they study the size of the basins of attractions of real Newton maps on the plane; finally, a recent article by the present author [De Leo, 2019] where some general conjecture is made based on analogy with the real one-dimensional case and on a significant experimental evidence.

Note that the numerical studies in [De Leo, 2019] aimed to provide a panoramic view as wide as possible of the dynamics of Newton maps on the real plane but were not meant (by any means) to be exhaustive. The main goal of the present article is exactly to study in detail a single case, the one of Newton maps of polynomial transformations of the plane into itself with both components quadratic, to show that, at least at the experimental level, all properties conjectured in [De Leo, 2019] hold for it. Incidentally, the present article has several points related to the works of Peitgen *et al.* but the points of view of our and their works is completely different. Finally we also point out that quadratic *complex* maps have also been the focus of an article by Hubbard and Papadopol [2008] and of the PhD thesis of Hubbard's pupil Roeder [2005].

The structure of the article is the following: in Sec. 2 we introduce all definitions and fundamental results we refer to in Sec. 3, where we present and

discuss our numerical results on the attractors and retractors of Newton maps associated to quadratic maps of the plane into itself. Ultimately, the numerical results in Sec. 3 suggest that all conjectures made in [De Leo, 2019] hold for this class of Newton maps.

2. Newton Maps

The concept of Newton map arises from the so-called Newton method, which is at the same time the most well-known method for solving numerically nonlinear systems of equations and one of the most important analytical tools to prove the existence of solutions to nonlinear equations in infinite-dimensional Banach spaces.

Definition 1. Let $F : D \subset B_1 \to B_2$, be a continuous map between the Banach spaces B_1 and B_2. We call *Newton map* associated to F the map $N_F : E \subset B_1 \to B_2$ defined by

$$N_F(x) = x - [F'(x)]^{-1}(F(x)),$$

where E is the subset of B_1 over which the Fréchet derivative $F'(x)$ exists and is invertible.

Clearly all zeros of F are fixed points for N_F. Newton's method is based on the fact that all such points are attracting (in fact, super-attracting when F is a Morse function), so that the iterates of any point "close enough" to a root of F will converge to it:

Theorem 1 [Kantorovich, 1949]. *Let $F : D \subset B_1 \to B_2$, be a continuous map between the Banach spaces B_1 and B_2 and assume that*:

(1) *F is Fréchet differentiable over some open convex subset $D_0 \subset D$;*
(2) *F' is Lipschitz on D_0.*

Then, for every $x_0 \in D_0$ such that $[F'(x_0)]^{-1}$ exists and is defined on the whole B_2, there is a neighborhood S of x_0 and an isolated root x_* of F such that $\lim_{n\to\infty} N_F^n(x) = x_* \in S$ for every $x \in S$.

As it often happens in Mathematics, Newton's method was not really first introduced by Isaac Newton but rather arose naturally from the works of several authors, including of course Newton himself — the interested reader is referred to the review article by Ypma [1995] for a detailed discussion on the history of this method. According to Ypma, the first appearance in literature of the Newton method in the form above, formulated for the one-dimensional real case only, goes back to the *Traité de la résolution des équations numériques* [Lagrange, 1798], published by Lagrange in 1798, while the above generalization to Banach spaces by Kantorovich arrived only 151 years later [Kantorovich, 1949].

The point of view of discrete dynamics is, in some sense, complementary with respect to the Kantorovich theorem, namely its main question is what happens to the iterates under N_F when the starting point is *far enough* from every root of F. The following concepts and theorems are central in this regard.

Definition 2. Let M be a compact manifold with a measure μ and f a surjective continuous map of a manifold M into itself. The ω-limit of a point $x \in M$ under f is the (closed) set of all points to whom x iterates are eventually close, namely

$$\omega_f(x) = \bigcap_{n\geq 0} \overline{\bigcup_{m\geq n} \{f^m(x)\}},$$

while its α-limit is the (closed) set of points to whom x iterated counterimages are eventually close, namely

$$\alpha_f(x) = \bigcap_{n\geq 0} \overline{\bigcup_{m\geq n} \{f^{-m}(x)\}}.$$

The ω- and α-limits of a set is the union of the ω- and α-limits of all of its points. The *forward* (resp., *backward*) *basin* $\mathcal{F}_f(C)$ (resp., $\mathcal{B}_f(C)$) under f of a closed invariant subset $C \subset M$ is the set of all $x \in M$ such that $\omega_f(x) \subset C$ (resp., $\alpha_f(x) \subset C$). Following Milnor [1985], we say that a closed subset $C \subset M$ is an *attractor* (resp., *repellor*) for f if:

(1) $\mathcal{F}_f(C)$ (resp., $\mathcal{B}_f(C)$) has strictly positive measure;
(2) there is no closed subset $C' \subset C$ such that $\mathcal{F}_f(C)$ (resp., $\mathcal{B}_f(C)$) coincides with $\mathcal{F}_f(C')$ (resp., $\mathcal{B}_f(C')$) up to a null set.

Definition 3. Given a compact manifold M and a continuous map $f : M \to M$, the *Fatou set* $F_f \subset M$ of f is the largest open set over which the family of iterates $\{f^n\}$ is *normal*, namely the largest open set over which there is a subsequence of the iterates of f that converges locally uniformly. The complement of F_f in M is the *Julia set* J_f of f. Finally, we denote by Z_f the set of points $x \in M$ where the Jacobian $D_x f$ is degenerate.

Definition 4. An Iterated Function System (IFS) $\mathcal{I}$ on a metric space (X, d) is a semigroup generated by some finite number of continuous functions $f_i : X \to X$, $i = 1, \ldots, n$. We say that $\mathcal{I}$ is *hyperbolic* when f_i are all contractions. The Hutchinson operator associated to $\mathcal{I}$ is defined as $\mathcal{H}(A) = \bigcup_{i=1}^{n} f_i(A)$, $A \subset X$.

Theorem 2 [Hutchinson, 1981; Barnsley & Demko, 1985]. *Let $\mathcal{I}$ be a hyperbolic IFS on X. Then there exists a unique nonempty compact set $K \subset X$ such that $\mathcal{H}(K) = K$. Moreover, $\lim_{n\to\infty} \mathcal{H}^n(A) = K$ for every nonempty compact set $A \subset X$.*

Theorem 3 [Barnsley, 1988]. *Let (Y, d) be a complete metric space and X a compact nonempty proper subset of Y. Denote by $\mathcal{K}(X)$ the set of the nonempty compact subsets of X endowed with the Hausdorff distance h (recall that h makes $\mathcal{K}(X)$ a complete metric space). Assume that one of the following conditions is satisfied*:

(1) *$f : X \to Y$ is an open map such that $f(X) \supset X$;*
(2) *$f : Y \to Y$ is an open map such that $f(X) \supset X$ and $f^{-1}(X) \subset X$.*

Then the map $F : \mathcal{K}(X) \to \mathcal{K}(X)$ defined by $F(K) = f^{-1}(K)$ is continuous, $\{F^n(K)\}$ is a Cauchy sequence, its limit $K_0 = \lim F^n(X) \in \mathcal{K}(X)$ is a repellor for f and it is equal to the set of points that never leave X under the action of f.

The main result on the dynamics of real Newton maps is the following result by Barna [1953] in one dimension:

Theorem 4 [Barna, 1953]. *Let p be a generic real polynomial of degree $n \geq 4$ without complex roots and denote its roots by $r_1, \ldots, r_n$. Then*:

(1) *$F_{N_p} = \bigcup_{i=1}^{n} \mathcal{F}(c_i)$;*
(2) *F_{N_p} has full Lebesgue measure;*
(3) *N_p has no attractive k-cycles with $k \geq 2$;*
(4) *N_p has repelling k-cycles of any order $k \geq 2$;*
(5) *J_{N_p} is equal, modulo a countable set, to a Cantor set $\mathcal{E}_{N_p}$ of Lebesgue measure zero.*

In 1984, this result was independently generalized by several authors in three different directions:

Theorem 5 [Wong, 1984]. *A sufficient condition for Barna's theorem to hold is that the polynomial p has no complex root and at least four distinct real roots, possibly repeated.*

Theorem 6 [Saari & Urenko, 1984]. *Let p be a generic polynomial of degree $n \geq 3$, A_p the collection of all bounded intervals in $\mathbb{R}\backslash Z_p$ and $\mathcal{A}_p$ the set of all sequences of elements of A_p. Then the restriction of N_p to the Cantor set $\mathcal{E}_{N_p}$ is semiconjugate to the one-sided shift map S on $\mathcal{A}_f$, namely there is a surjective homomorphism $h_p : \mathcal{E}_{N_p} \to A_p$ such that $T \circ h_p = h_p \circ N_p$.*

Theorem 7 [Hurley & Martin, 1984]. *Let p be a generic polynomial of degree $n \geq 3$. Then N_p has at least $(n-2)^k$ k-cycles for each $k \geq 1$ and the topological entropy of N_p is at least $\log(n-2)$.*

In our knowledge, no further generalization of Barna's result has been published since the three above and no general theorem has been proved for Newton maps coming from real maps in more than one dimension. In a recent article [De Leo, 2019], based on several numerical observations and in analogy with Barna's theorem, we posed the following "simple dynamics" conjectures for the two-dimensional case:

Definition 5. We say that a point p of the Julia set J_F of a rational map $F : \mathbb{R}^2 \to \mathbb{R}^2$ is *regular* if there is a neighborhood U of p such that $J_F \cap U$ is a connected one-dimensional submanifold and U contains points from two different basins.

Conjecture 1. *Let $f : \mathbb{R}^2 \to \mathbb{R}^2$ be a generic polynomial map of degree $n \geq 3$. Then there is some nonempty open subset $A \subset f(\mathbb{RP}^2)$ such that $\alpha_{N_f}(x)$ is equal to the set of nonregular points of the boundary of J_{N_f} for all $x \in A$.*

Conjecture 2. *Let $f : \mathbb{R}^2 \to \mathbb{R}^2$ be a polynomial map of degree $n \geq 3$ with n distinct real roots $\{c_i\}$. Then*:

(1) *J_{N_f} is the countable union of wedge sums of countable number of circles and of Cantor sets of circles of measure zero;*
(2) *F_{N_f} has no wandering domains;*
(3) *the union of the basins of attraction $\mathcal{F}_{N_f}(c_i)$ has full Lebesgue measure;*
(4) *every neighborhood of any point of J_{N_f} contains points from at least two distinct basins of attractions;*
(5) *unlike the holomorphic case*:
   (a) *basins of attractions are not necessarily simply connected;*
   (b) *immediate basins of attraction are not necessarily unbounded;*

(c) *J_{N_f} can have interior points without being equal to the whole $\mathbb{RP}^2$.*

In the next two sections we study numerically in some detail the dynamics of the Newton maps of two of the simplest families of polynomial homomorphisms of the plane. Our results fully support both our conjectures.

In the remainder of this section we recall some well known properties of the Newton maps (e.g. see [Hubbard & Papadopol, 2008; Hubbard & Hubbard, 2015]) that we will use below.

Let (x^α), $\alpha = 1, \ldots, n$, be a coordinate system in $\mathbb{K}^n$, where $\mathbb{K} = \mathbb{R}$ or $\mathbb{C}$, and let us denote by f^{a}, $\mathrm{a} = 1, \ldots, n$, the components of the map $f : \mathbb{K}^n \to \mathbb{K}^n$, by $\partial_\alpha f^{\mathrm{a}}$ the entries of its Jacobian matrix and by $\partial_{\mathrm{a}} \overline{f}^\alpha$ those of the Jacobian of f's inverse, namely the inverse matrix of $(\partial_\alpha f^{\mathrm{a}})$. Then, in coordinates, the components of N_f are given by

$$N_f^\alpha(x) = x^\alpha - \partial_{\mathrm{a}} \overline{f}^\alpha(x) f^{\mathrm{a}}(x).$$

Proposition 1. *The entries of the Jacobian matrix $D_x N_f$ are given by*

$$\partial_\gamma N_f^\alpha(x) = \partial_b \overline{f}^\alpha(x) \partial^2_{\beta\gamma} f^b(x) \partial_{\mathrm{a}} \overline{f}^\beta(x) f^{\mathrm{a}}(x).$$

Proof. A direct calculation shows that

$$\begin{aligned}\partial_\gamma N_f^\alpha &= \partial_\gamma(x^\alpha - \partial_{\mathrm{a}} \overline{f}^\alpha f^{\mathrm{a}}) \\ &= \delta^\alpha_\gamma - \partial_\gamma(\partial_{\mathrm{a}} \overline{f}^\alpha) f^{\mathrm{a}} - \partial_{\mathrm{a}} \overline{f}^\alpha \partial_\gamma f^{\mathrm{a}}.\end{aligned}$$

Since

$$\partial_\alpha f^{\mathrm{a}} \partial_{\mathrm{a}} \overline{f}^\beta = \delta^\beta_\alpha,$$

then

$$\partial^2_{\gamma\alpha} f^{\mathrm{a}} \partial_{\mathrm{a}} \overline{f}^\beta + \partial_\alpha f^{\mathrm{a}} \partial_\gamma(\partial_{\mathrm{a}} \overline{f}^\beta).$$

Hence

$$\partial_\gamma(\partial_{\mathrm{a}} \overline{f}^\alpha) = -\partial_{\mathrm{a}} \overline{f}^\beta \partial^2_{\gamma\beta} f^b \partial_b \overline{f}^\alpha$$

and the claim follows. ■

Corollary 1. *The set $Z_f = \{x \in KP^n \,|\, \det D_x N_f = 0\}$ of all degenerate points of N_f is given by all points x such that the matrix*

$$(A^b_\gamma) = (\partial^2_{\gamma\beta} f^b(x) \partial_{\mathrm{a}} \overline{f}^\beta(x) f^{\mathrm{a}}(x))$$

is degenerate. Equivalently, Z_f is the set of all x such that either $f(x) = 0$ or the vector $\partial_b \overline{f}^\alpha(x) f^{\mathrm{a}}(x)$ is a critical direction of the quadratic map $v^\alpha \mapsto \partial^2_{\gamma\beta} f^{\mathrm{a}}(x) v^\gamma v^\beta$.

Points where DN_f is degenerate play an important role in the dynamics of N_f, for example, in the one-dimensional case J_{N_f} is equal to $\alpha_f(Z_f)$. Moreover, the fact that DN_f is identically zero at every root of f gives us immediately the following fundamental property:

Corollary 2. *All simple roots of f are super-attractive fixed points for N_f.*

Remark 1. Note that, while in the one-dimensional case the fixed point at infinity of a polynomial is always repelling, fixed points at infinity in the multidimensional case can be attractive (e.g. see Example 4 in [De Leo, 2019]).

Proposition 2. *If $\psi, \phi : \mathbb{K}^n \to \mathbb{K}^n$ are, respectively,* affine *and* linear *automorphisms of $\mathbb{K}^n$, namely $\psi^\alpha(x) = A^\alpha_\beta x^\beta + u^\alpha$ and $\phi^{\mathrm{a}}(y) = B^b_{\mathrm{a}} y^{\mathrm{a}}$ for some $A, B \in GL_n(\mathbb{K})$ and $u, v \in \mathbb{K}^n$, then*

$$N_{\phi \circ f \circ \psi} = \psi^* N_f$$

namely the Newton map N_f has the same dynamics as $N_{\phi \circ f \circ \psi}$.

Proof. In this case $\partial_\beta \psi^\alpha = A^\alpha_\beta$ and $\partial_b \phi^{\mathrm{a}} = B^{\mathrm{a}}_b$, so that

$$\begin{aligned}&\psi^* N_f^\alpha(x) \\ &\quad = \overline{A}^\alpha_\beta [N_f^\beta(Ax + b) - b^\beta] \\ &\quad = \overline{A}^\alpha_\beta [A^\beta_\gamma x^\gamma + b^\beta - \partial_b \overline{f}^\beta|_{Ax+b} f^b(Ax + b) - b^\beta] \\ &\quad = \delta^\alpha_\gamma x^\gamma - \overline{A}^\alpha_\beta \partial_b \overline{f}^\beta|_{Ax+b} \overline{B}^b_{\mathrm{a}} B^{\mathrm{a}}_c f^c(Ax + b) - b^\beta \\ &\quad = x^\alpha - \partial_{\mathrm{a}}(\overline{\phi \circ f \circ \psi})^\alpha(x)(\phi \circ f \circ \psi)^{\mathrm{a}}(x) \\ &\quad = N^\alpha_{\phi \circ f \circ \psi}(x)\end{aligned}$$

since

$$\begin{aligned}\partial_{\mathrm{a}}(\overline{\phi \circ f \circ \psi})^\alpha(x) &= \partial_{\mathrm{a}}(\overline{\psi} \circ \overline{f} \circ \overline{\phi})^\alpha(x) \\ &= \partial_{\mathrm{a}} \overline{\phi}^b \partial_b \overline{f}^\beta|_{Ax+b} \partial_\beta \overline{\psi}^\alpha.\end{aligned}$$

■

Definition 6. Let $f = (p, q) \in C^k(\mathbb{R}^2, \mathbb{R}^2)$. We call *pencil* $\mathcal{P}_f$ associated to f the linear subspace of $C^k(\mathbb{R}^2)$ generated by p and q. If p and q are polynomials, by *type* of the pencil, denoted by $\tau(\mathcal{P}_f)$, we mean the pair of the highest and lowest degrees of polynomials in the pencil.

Thanks to Proposition 2, we can replace the components of a Newton map N_f with any two independent linear combination of them without

altering its dynamics, so what really counts is the pencil of its components rather than the components themselves.

3. Dynamics of Newton Maps of Quadratic Maps

We consider maps $f = (p, q) : \mathbb{R}^2 \to \mathbb{R}^2$ where both p and q are quadratic polynomials in x, y in general position. Hubbard and Papadopol [2008] showed that, in the complex case, one can reduce this problem to the study of the Newton maps N_g with

$$g(x, y) = (y - x^2, (x - x_0) - (y - y_0)^2), \quad (x_0, y_0) \in \mathbb{C}^2.$$

As to be expected in the real case we have, instead, two distinct cases:

Proposition 3. *Let $f(x, y) = (p(x, y), q(x, y)) : \mathbb{R}^2 \to \mathbb{R}^2$, with p and q quadratic polynomials in generic position. Then N_f is smoothly conjugated to N_g, where $g(x, y)$ has one of the following two forms*:

(1) $\mathfrak{f}_{x_0,y_0}(x, y) = (y - x^2, (x - x_0) - (y - y_0)^2)$, $x_0 \geq 0$, $y_0 \in \mathbb{R}$;
(2) $\mathfrak{f}_{x_0,y_0;a}(x, y) = (xy - 1, (x - x_0)^2 - a(y - y_0)^2 - 1)$, $y_0 \geq x_0 \geq 0, a > 0$.

Proof. We say that a quadratic polynomial is elliptic, hyperbolic or parabolic depending on the type of its generic level set. Through an affine transformation, we can always reduce p to one of the following quadratic polynomials:

(1) $\mathfrak{c}(x, y) = x^2 + y^2 - 1$ (elliptic);
(2) $\mathfrak{h}(x, y) = xy - 1$ (hyperbolic);
(3) $\mathfrak{p}(x, y) = y - x^2$ (parabolic).

When p is elliptic, given the rotational symmetry of the circle, we can always find a second affine transformation that reduces q to one of the following quadratic polynomials:

(a) $q_e(x, y) = a(x - x_0)^2 + b(y - y_0)^2 - 1$, with $y_0 \geq x_0 \geq 0$ and $a > b > 0$;
(b) $q_h(x, y) = a(x - x_0)^2 - b(y - y_0)^2 - 1$, with $y_0 \geq x_0 \geq 0$ and $a > b > 0$;
(c) $q_p(x, y) = y - y_0 - a(x - x_0)^2$, with $a > 0$, $x_0 \geq 0$ and $y_0 \in \mathbb{R}$.

In the first two cases we can easily find two linear combinations that give us two parabolic polynomials, in the last case we can use q_p to cancel one of the two quadratic terms of $\mathfrak{c}$. In all three cases then we can find an affine map ψ and a linear map ϕ such that $f = \phi \circ \hat{f} \circ \psi$ where both components of $\hat{f}$ are parabolic. With yet another affine transformation, we can finally transform $\hat{f}$ in the final form $\mathfrak{f}_{x_0,y_0}$, namely N_f is conjugated to $N_{\mathfrak{f}_{x_0,y_0}}$.

When p is hyperbolic, we can assume that q is either parabolic or hyperbolic (the elliptic case is covered above). In the first case, $q(x, y) = ax^2 + 2bxy + cy^2 + \ell(x, y)$, where ℓ is linear and $ac - b^2 = 0$. By adding $2\lambda xy$ to q we get a parabola if and only if $ac - (b + \lambda)^2 = 0$, namely $\lambda = 0, -2b$, so again we reduce to the case of two parabolic polynomials and so to $\mathfrak{f}$. In the second case, $q(x, y) = ax^2 + 2bxy + cy^2 + \ell(x, y)$ with $ac - b^2 < 0$. After adding $2\lambda xy$ to q, its type is determined by the sign of $d(\lambda) = ac - (b + \lambda)^2 = ac - b^2 - 2b\lambda - \lambda^2$. Since the discriminant of $d(\lambda)$ is $4ac$, the sign of d is strictly negative for all λ when a and c have opposite signs. In this case, therefore, all linear combinations of p and q are hyperbolic and N_f is conjugate to some $N_{\mathfrak{f}_{x_0,y_0;a}}$. ■

Definition 7. We denote respectively by $\mathbf{N}_{x_0,y_0}$ and $\mathbf{N}_{x_0,y_0;a}$ the Newton maps associated to $\mathfrak{f}_{x_0,y_0}$ and $\mathfrak{f}_{x_0,y_0;a}$ and, analogously, we use the symbols $\mathbf{J}_{x_0,y_0}$, $\mathbf{J}_{x_0,y_0;a}$, $\mathbf{Z}_{x_0,y_0}$ and $\mathbf{Z}_{x_0,y_0;a}$ for their Julia sets and for the sets of degeneracy of their Jacobians.

Below we present our numerical analyses of some Newton maps $\mathbf{N}_{x_0,y_0}$ and $\mathbf{N}_{x_0,y_0;a}$ and compare it against our conjectures. We focus on the basins of attraction and of retraction of those Newton maps. We obtain the first by considering a regular lattice of points inside a square (of the order of $10^3 \times 10^3$ points), evaluating the iterates of all such points under those maps and assigning to each point different colors depending on which root of the corresponding quadratic polynomial map they appear to converge. We obtain the second by choosing an arbitrary point *within a suitable open set*, evaluating its backward iterates until some fixed recursion order (usually between 10 and 20) and plotting all points obtained at the last recursion step.

3.1. *The map* $\mathbf{N}_{0,0}$

The Newton map

$$\mathbf{N}_{0,0} = \left(y\frac{2x^2 + y}{4xy - 1}, x\frac{2y^2 + x}{4xy - 1} \right)$$

was first studied, in this context, in great detail by Peitgen *et al.* [1988, 1989] and later, in the complex

setting, by Hubbard *et al.* [2001]. In homogeneous coordinates, this map writes as

$$[x : y : z] \to [y(2x^2 + yz) : x(2y^2 + zx) : z(4xy - z^2)],$$

from which it can be seen that $\mathbf{N}_{0,0}$ has the following three points of indeterminacy: one bounded, $[1 : 1 : -2]$, and two at infinity, $[1 : 0 : 0]$ and $[0 : 1 : 0]$. The restriction of $\mathbf{N}_{0,0}$ to the circle at infinity, where defined, is the identity. On each point at infinity, the eigenvalues of $D\mathbf{N}_{0,0}$ are equal to 1 in the direction tangent to infinity and to 2 in the eigendirection transversal to it, namely the points at infinity where $D\mathbf{N}_{0,0}$ is defined are all repelling with respect to points lying outside of the circle at infinity. Nevertheless, the iterates of the points on the half-lines $\{x = 0, |y| > 1\}$ and $\{|x| > 1, y = 0\}$ diverge while bouncing back and forth between the two half-lines just as if $[1 : 0 : 0]$ and $[0 : 1 : 0]$ were an attracting cycle — this is not a contradiction because $\mathbf{N}_{0,0}$ is not defined at these points.

Rational maps of degree three can have at most six invariant lines. As Hubbard and Papadopol showed in [2008], in the complex case the Newton map of a generic polynomial map with quadratic components has the maximal number of invariant lines, namely the lines joining all pairs of its four roots, and it restricts on each such line to the one-dimensional Newton method for a quadratic polynomial in one variable with those roots. Correspondingly, in the real case the invariant (real) lines are all those joining pairs of distinct roots plus, in case not all roots are real, the intersections with the real plane of the complex lines passing through pairs of distinct complex roots with nonzero imaginary part. For such a generic map therefore there will be exactly six invariant straight lines when all roots are real and only two otherwise. In this last case, we call *ghost line* the invariant one that does not contain any root. Hence there will be a single ghost line when there are two real and two complex-conjugate roots and two ghost lines when there are two pairs of complex-conjugate roots.

The two lines invariant under $\mathbf{N}_{0,0}$ are the bisectrix of the first and third quadrants, joining the two real roots, and the ghost line $\ell = \{y + x + z = 0\}$, intersection with the real plane of the complex line passing through the two complex roots $e^{2\pi i/3}$ and $e^{4\pi i/3}$ [in brown in Fig. 2(top, left)]. $\mathbf{N}_{0,0}$ restricts on ℓ to the Newton map of the polynomial $p(x) = x^2 + x + 1$ and, correspondingly to the absence of real roots of this polynomial, J_p is the whole line and N_p has nontrivial repelling cycles, for instance $N_p(0) = -1$ and $N_p(-1) = 0$. On the bisectrix, instead, it coincides with the Newton map of the polynomial $q(x) = x^2 - x$, whose dynamics, correspondingly to the fact that q has a maximal number of real roots, is known to be trivial: its Julia set is the single point $x = 1/2$, the only point where N_q' is zero. This point, that has no counterimages, separates the two basins of attraction of the two roots. In particular, N_q has no nontrivial cycles.

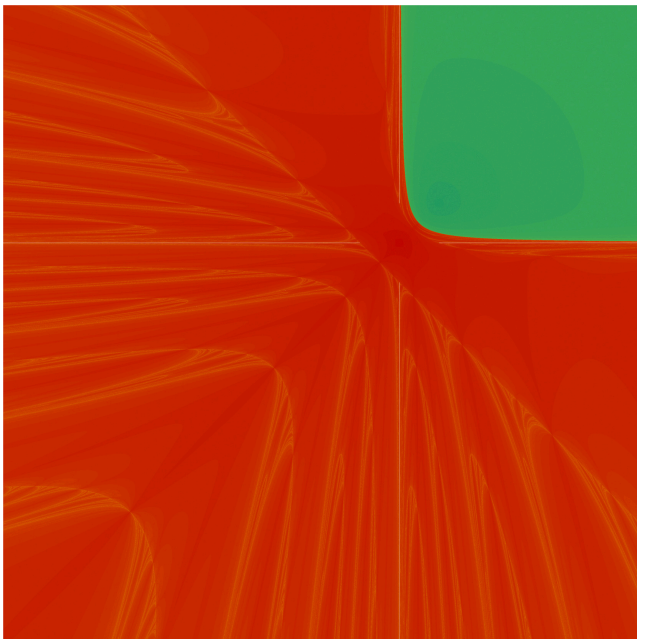

Fig. 1. Basins of attraction of $\mathbf{N}_{0,0}$ in the rectangle $[-6, 10] \times [-10, 6]$. The only real roots of $\mathfrak{f}_{0,0}$ are the points $(0, 0)$ (whose basin is colored in red) and $(1, 1)$ (in green). The yellow points are those for which the Newton method converges only after a large number of iterations — as the numerical and analytical data shown in Fig. 2 suggest, these are all points belonging to the counterimages of $\mathbf{Z}_{0,0}$. Lighter tints correspond to higher convergence time.

Now, let $C = \{(x, y) \,|\, y > x^2 \text{ or } x > y^2\}$ [white region in Fig. 2(top, left)], denote the two disjoint connected components of $\mathbb{R}^2 \backslash C$ by A (the one contained in the first quadrant) and B, by C_0 and C_1 the two disjoint connected components of $C \backslash \mathbf{Z}_{0,0}$ having at their boundary respectively the roots $(0, 0)$ and $(1, 1)$ and by $D \subset B$ the half-plane below the invariant line ℓ. The (formal) counterimages of a point (x_0, y_0) are the four points $w_{m,n} = (x_0 + (-1)^m \sqrt{x_0^2 - y_0}, y_0 + (-1)^n \sqrt{y_0^2 - x_0})$, $m, n = 0, 1$, so that:

(1) $\mathbf{N}_{0,0}(\mathbb{R}^2) = A \sqcup B$;
(2) $\mathbf{N}_{0,0}(C_1) \subset A$, $\mathbf{N}_{0,0}(C_0) \subset B$;

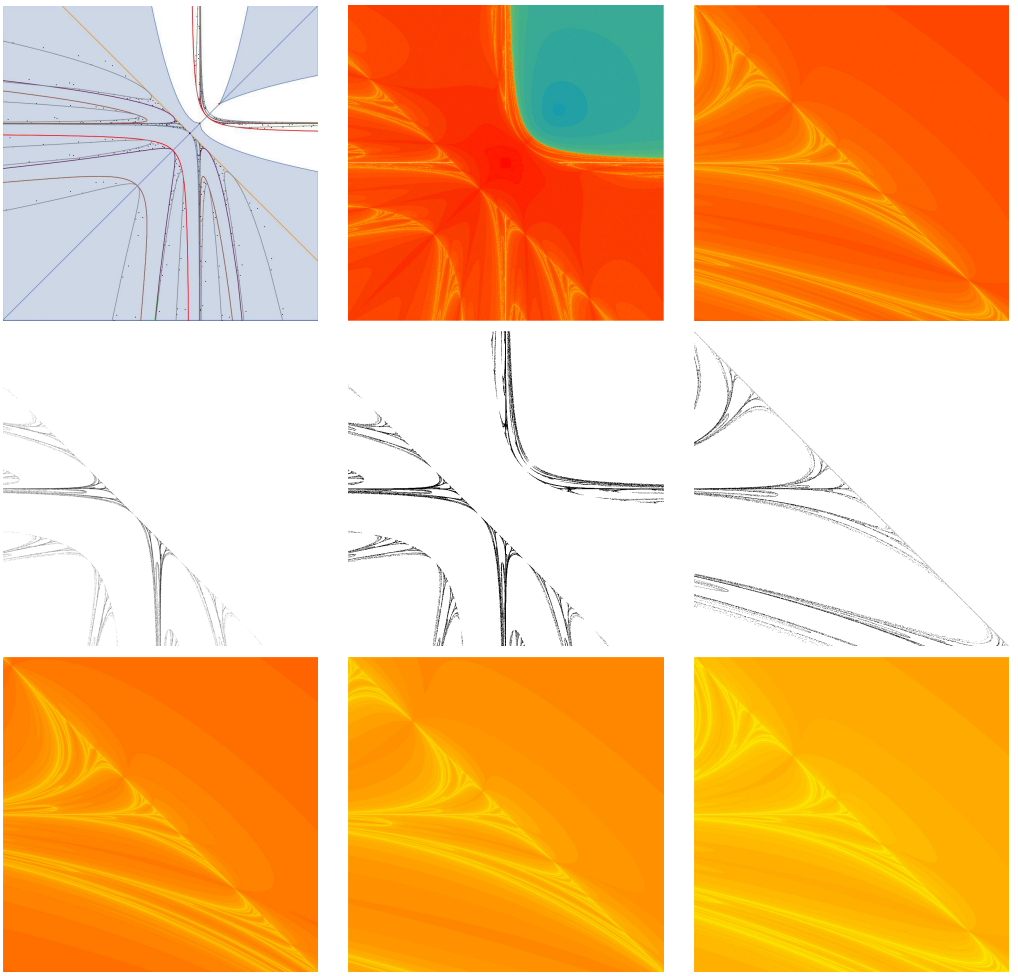

Fig. 2. (Top, left) Fixed points (red), indeterminacy point (blue) and invariant lines of $\mathbf{N}_{0,0}$ and set $\mathbf{Z}_{0,0}$ together with some of their counterimages: the ghost line is in orange and its first and second counterimages in red and brown respectively, $\mathbf{Z}_{0,0}$ in light blue and its counterimages in purple and gray. The black points are the counterimages via $\mathbf{N}_{0,0}$ of a single point of the plane up to the fifth level of iteration. (Top, center & right) Basins of attraction and Julia set of $\mathbf{N}_{0,0}$ in the rectangles $[-3,3]^2$ and $[0.95,1.05]\times[-0.05,0.05]$. (Center) Approximations of $\mathbf{J}_{0,0}$ obtained as the first $3\cdot10^5$ points of a random backward orbit (left) and as the points of the set $\mathbf{N}_{0,0}^{-11}(1,-3.6)$ (center, right). (Bottom) Basins and Julia set of $\mathbf{N}_{0,0}$ in the squares of side respectively 10^{-3} (left), 10^{-4} (center) and 10^{-5} centered at $(-1,0)$. Lighter colors correspond to higher convergence time.

(3) three of the counterimages of each point in the interior of A belong to C and one to A;
(4) the counterimages of each point in the interior of B belong to $B\cup C$ and no more than two belong to C;
(5) the three counterimages $w_{1,0}, w_{0,1}, w_{1,1}$ of each point of D belong to D and the fourth to C_0.

The branch of $\mathbf{Z}_{0,0}$ in the first quadrant is the boundary between the two basins, while the other one is tangent at $[1:1:-2]$ to ℓ. Some other component of the Julia set of $\mathbf{N}_{0,0}$ is plotted in Fig. 2(top, left). The counterimage of ℓ under $\mathbf{N}_{0,0}$ has three connected components, namely ℓ itself and the two red curves, one inside C and one inside A. The one in C of course has no counterimage while the one in A has four of them, plotted in brown, three of which inside A and one inside C. Similarly, the branch of $\mathbf{Z}_{0,0}$ in C has no counterimage while the other one has four, plotted in purple, three of which inside A and one inside C. Moreover, two of them (corresponding to the solutions w_{00} and w_{11}) are tangent to the two nontrivial counterimages of ℓ while the other two are tangent to ℓ. In the limit, infinitely many components of $\mathbf{J}_{0,0}$ will be tangent to ℓ, forming a shape similar to the delta of a river on the shore represented by the straight line. The numerical evidence therefore suggests that, just as in the complex case, $\mathbf{J}_{0,0}$ is the α-limit of $Z_{0,0}$.

Another way of looking at $\mathbf{J}_{0,0}$ is through Theorem 3. Let U be a small enough neighborhood of the boundary of C and set $X = \mathbb{RP}^2 \backslash U$. Then $\mathbf{N}_{0,0}(X) \supset X$, since every point inside U has a counterimage in $A \sqcup B$ (take $w_{0,0}$ for points in $U \cap A$ and $w_{1,1}$ for points in $U \cap B$), and it is an open map on X because we are away from the zeros of the radicands. Hence $\lim_{n\to\infty} \mathbf{N}_{0,0}^{-n}(X)$ defines a repellor for $\mathbf{N}_{0,0}$ which is exactly the set of points that do not leave X under $\mathbf{N}_{0,0}$ (see [Barnsley, 1988]). In Fig. 2(center), we show the set $\mathbf{N}_{0,0}^{-11}(10, -3.6)$, suggesting that the counterimage of a single point, rather than the whole X, can be enough to give the whole $\mathbf{J}_{0,0}$. Numerical experiments also show that every point of B gives rise to similar counterimage sets while the corresponding sets for points in A are empty — in this case indeed the only counterimage of each point lying in A goes to infinity. Now, since the Julia set is invariant and numerical evidence suggests that the only attractors of $\mathbf{N}_{0,0}$ are the roots of f, the only points that leave X are those in the basins of attractions of the two roots and so it must be $\mathbf{J}_{0,0} = \lim_{n\to\infty} \mathbf{N}_{0,0}^{-n}(X)$. Notice that the presence of points of indeterminacy inside X is not a problem because these singularities can be eliminated by blow-ups [Hubbard & Papadopol, 2008].

A third way is to see $\mathbf{J}_{0,0}$ as the invariant compact set of the IFS $\mathcal{I}$ generated by the restriction of the maps $\{w_{10}, w_{01}, w_{11}\}$ to the set $D = \{x + y \leq -1\} \subset B$. Indeed D is invariant under the action of $\mathcal{I}$ and

$$w_{10}(D) \cup w_{01}(D) \cup w_{11}(D) = \mathbf{N}_{0,0}^{-1}(D) \cap D$$

so that the Hutchinson operator $H(S) = w_{10}(S) \cup w_{01}(S) \cup w_{11}(S)$, $S \subset D$ associated to this IFS, based on the discussion in the previous paragraph, has a fixed point given by $K = \lim_{n\to\infty} \mathbf{N}_{0,0}^{-n}(D) = \mathbf{J}_{0,0} \cap D$. Note that this point of view also suggests that the component of $\mathbf{J}_{0,0}$ inside C is simply $w_{00}(K)$, namely $\mathbf{J}_{0,0} = K \sqcup w_{00}(K)$.

Again, by Theorem 3, this is precisely the set of points that do not converge to $(0, 0)$. The picture of the Julia set in black and white in Fig. 2(center, left) has been obtained by plotting the first $3 \cdot 10^5$ points of a random backward orbit of the point $(3, -3.6)$ and the picture does not appear to depend on the initial point taken within the set B. On the contrary, backward orbits starting in A diverge to infinity. We are not aware of any systematic investigation of this fractal and, in particular, it is unknown whether its measure is zero or not and what its Hausdorff dimension might be.

3.2. *The map* $\mathbf{N}_{-2,2}$

The map $\mathfrak{f}_{-2,2}$ has four roots, namely the points $p_1 = (-1, 1)$, $p_2 = (2, 4)$, $p_3 \simeq (-1.62, 2.62)$ and $p_4 \simeq (0.62, 0.38)$. Its Newton map is

$$\mathbf{N}_{-2,2} = \left(\frac{2x^2y + y^2 - 4x^2 - 1}{4xy - 8x - 1}, x \frac{2y^2 + x - 4}{4xy - 8x - 1} \right),$$

namely, in homogeneous coordinates,

$$[x : y : z] \to [2x^2y + y^2z - 4x^2z - z^3 : x(2y^2 + xz - 4z^2) : z(4xy - 8xz - z^2)].$$

In this case we have five points of indeterminacy: three bounded, namely $[-1, 3, 2]$, $[-7 - 3\sqrt{5} : 1 + 3\sqrt{5} : 4]$ and $[-7 + 3\sqrt{5} : 1 - 3\sqrt{5} : 4]$, and two unbounded, namely $[1 : 0 : 0]$ and $[0 : 1 : 0]$.

Fig. 3. Basins of attraction of $\mathbf{N}_{-2,2}$ in the square $[-10, 10]^2$. The four real roots of g are the points $(0, 0)$, $(2, 4)$ and, approximately, $(-1.62, 2.62)$ and $(0.62, 0.38)$ and each basin corresponds to a different color. In this picture, it is possible to see a qualitative difference among the boundary points of the basins: the ones between the orange and the light blue regions close to the symmetry axis of the basins and the ones close to the nodal point on the same axis are regular, namely a small enough neighborhood of them is cut by the boundary in just two regions; all others instead seem irregular, namely each of their neighborhood intersects infinitely many basin components. Darker shades correspond to higher convergence time.

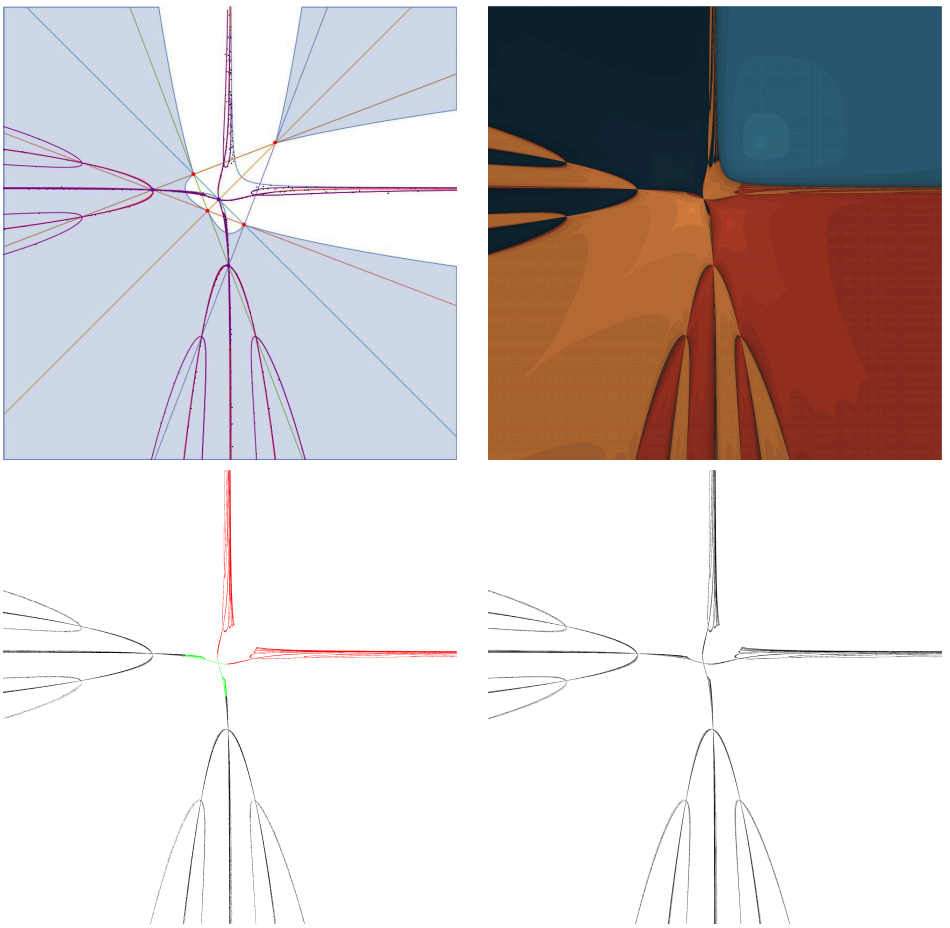

Fig. 4. (Top, left) Some important elements of the dynamics of $\mathbf{N}_{-2,2}$ in the square $[-10,10]^2$: fixed points (red), indeterminacy points (blue), the six invariant lines, the set $Z_{-2,2}$ (light blue) and its first two counterimages (resp., red and purple). The shaded region is $\mathbf{N}_{-2,2}(\mathbb{R}^2)$ and the black points are the counterimages via $\mathbf{N}_{-2,2}$ of a single point of the plane up to the fifth level of iteration. (Top, right) Basins of $\mathbf{N}_{-2,2}$ in the square $[-10,10]^2$. (Bottom, left) First $3\cdot 10^5$ points of a random backward orbit of a point below the light blue invariant line under the three branches $w_{1,0}, w_{0,1}, w_{1,1}$ of $\mathbf{N}_{-2.2}$ (in black). Notice that there is a small white open set below the line. When the orbit falls there we paint the point in green and choose a different counterimage. The red points are the images of the black points under $w_{0,0}$. (Bottom, right) This picture shows the set $\mathbf{N}_{-2,2}^{-13}(-20,-1.4)$. These two bottom pictures strongly suggest that through α-limits we can only get the set of irregular points of the Julia set.

Just like in the previous case, the restriction of $\mathbf{N}_{-2,2}$ to the circle at infinity is the identity, where it is defined, and all these fixed points are repelling in the direction orthogonal to the circle at infinity. Corresponding to the four roots of $\mathfrak{f}_{-2,2}$, $\mathbf{N}_{-2,2}$ has six invariant lines on which it restricts to the Newton map of some quadratic polynomial in one variable [see Fig. 4(top, left)]. As for $\mathfrak{f}_{0,0}$, we set $\mathfrak{f}_{-2,2}(\mathbb{R}^2) = A \sqcup B$, with A the component contained in the first quadrant. We denote by C_0 and C_1 the two disjoint connected components of $C\backslash\mathbf{Z}_{-2,2}$ containing respectively the roots $(-1,1)$ and $(2,4)$ and by H the half-plane below the line $x+y=1$, joining the roots p_2 and p_3. The four (formal) preimages of a point (x_0,y_0) are given by $w_{m,n} = (x_0 + (-1)^m\sqrt{x_0^2 - y_0}, y_0 + (-1)^n\sqrt{(y_0-2)^2 - x_0 + 2})$, $m,n = 0,1$, and satisfy properties similar to those of f, namely:

(1) $\mathbf{N}_{-2,2}(\mathbb{R}^2) = A \sqcup B$;
(2) $\mathbf{N}_{-2,2}(C_1) \subset A$, $\mathbf{N}_{-2,2}(C_0) \subset B$;
(3) three of the counterimages of each point in the interior of A belong to C and one to A;
(4) three of the counterimages of each point of the interior of B belong to $B \cup H$ and one to C.

In Fig. 4(top, left), we show the four roots (in red) together with the lines joining them, the three bounded indeterminacy points (in blue), the region C (in white), the hyperbola $\mathbf{Z}_{-2,2}$ (in blue)

and its first two counterimages (resp., in red and purple) under N_f. The numerical evidence suggests that the α-limit of the set of points where $D\mathbf{N}_{-2,2}$ is degenerate coincides with the set of irregular points of $\mathbf{J}_{-2,2}$.

Now let U be a small enough neighborhood of C and set $X = \mathbb{RP}^2 \setminus U$. Then, similarly to what happens for $\mathbf{N}_{0,0}$, $\mathbf{N}_{-2,2}(X) \supset X$ and the restriction of $\mathbf{N}_{-2,2}$ to X is an open map. Hence $\lim_{n\to\infty} \mathbf{N}_{-2,2}^{-n}(X)$ defines a repellor for $\mathbf{N}_{-2,2}$ which is exactly the set of points that do not leave X under $\mathbf{N}_{-2,2}$. In Fig. 4(bottom, right), we show the set $\mathbf{N}_{-2,2}^{-13}(-20,-1.4)$, suggesting that this repellor coincides with the set of irregular points of $\mathbf{J}_{-2,2}$. As in the previous case, the counterimages of any point in B give similar results while the counterimages of points in A go to infinity.

Similarly to the previous case, we can get the set of irregular points of $\mathbf{J}_{-2,2}$ as the invariant compact set of the IFS $\mathcal{I}$ generated by the restriction of the maps $\{w_{10}, w_{01}, w_{11}\}$ to the set $D = \{x + y \leq 1\} \subset B$. In this case though $\mathcal{I}$ is not, strictly speaking, a well-defined IFS on D since there is a bounded open subset $N \subset D$ where the maps are not defined. Nevertheless it is reasonable to believe, supported by numerical experiments, that the concept of IFS can be extended to this type of maps and that a unique compact subset still exists. In Fig. 4(bottom, left), we show in black the first $3 \cdot 10^5$ points of a random backward orbit of $(3, -3.6)$ under $\mathcal{I}$; the green points are points that fell, during the backward iteration, in N, in which case we select a different random counterimage in order to keep going backwards; the red points are the image of the black ones under the map w_{00}. Numerical experiments suggest that the limits of such backward orbits do not depend on the initial point inside $D\setminus N$.

3.3. *The map* $\mathbf{N}_{-1,2}$

The Newton map

$$\mathbf{N}_{-1,2}(x,y) = \left(\frac{2x^2y + y^2 - 4x^2 - 3}{4xy - 8x - 1}, x\frac{2y^2 + x - 6}{4xy - 8x - 1}\right)$$

shares many characteristics with $\mathbf{N}_{0,0}$. Like $\mathbf{N}_{0,0}$, $\mathbf{N}_{-1,2}$ has two attracting fixed points $p_1 \simeq (-1.9, 3.7)$ and $p_2 \simeq (0.81, 0.65)$, corresponding to the two roots of $\mathfrak{f}_{-1,2}$ and three points of indeterminacy: one bounded, approximately $[-0.067 : -1.7 : 1]$, and two unbounded, namely $[1:0:0]$ and $[0:1:0]$. The restriction of $\mathbf{N}_{-1,2}$ to the circle at infinity is the identity, where defined, and all these fixed points are repelling in a direction transversal to the circle at infinity. Even in this case, $\mathbf{N}_{-1,2}(\mathbb{R}^2) = A \sqcup B$ and $Z_{-1,2}$ divides $C = \mathbb{R}^2 \setminus \mathbf{N}_{-1,2}(\mathbb{R}^2)$ into two open sets C_0 and C_1 so that $\mathbf{N}_{-1,2}(C_1) \subset A$, $\mathbf{N}_{-1,2}(C_0) \subset B$ and the half-space D below the ghost line is invariant under the first three of the inverse branches

$$w_{m,n} = (x_0 + (-1)^m\sqrt{x_0^2 - y_0}, \quad y_0 + (-1)^n\sqrt{(y_0-2)^2 - x_0 - 1}),$$

with $m, n = 0, 1$.

Unlike $\mathbf{N}_{0,0}$, though, $\mathbf{N}_{-1,2}$ shows evident signs of the presence of a third attractor $\mathcal{C}$, whose basin is shown in gold color in Fig. 5, lying on its ghost line. Numerics suggest that the dynamics on $\mathcal{F}(\mathcal{C})$ is chaotic (namely highly dependent on the initial point). In particular, this means that $\mathcal{F}(\mathcal{C}) \subset \mathbf{J}_{-1,2}$, suggesting furthermore that $\mathbf{J}_{-1,2}$ has nonempty interior and so a nonzero measure. Consistently with Conjecture 1, the numerical evaluation of the α-limits of points in B [Fig. 6(bottom, right)] and of the invariant set of the IFS generated by the maps $w_{1,0}, w_{0,1}, w_{1,1}$ [Fig. 6(bottom, left)] suggests that

Fig. 5. Basins of attraction of $\mathbf{N}_{-1,2}$ in the square $[-10, 10]^2$. The two real roots of $\mathfrak{f}_{-1,2}$ are the points $p_1 \simeq (1.9, 3.7)$ and $p_2 \simeq (0.81, 0.65)$ and the corresponding basins have been colored in cyan and red, respectively. The basin in gold corresponds to a chaotic attractor on the ghost line of $\mathbf{N}_{-1,2}$. Darker shades correspond to higher convergence time.

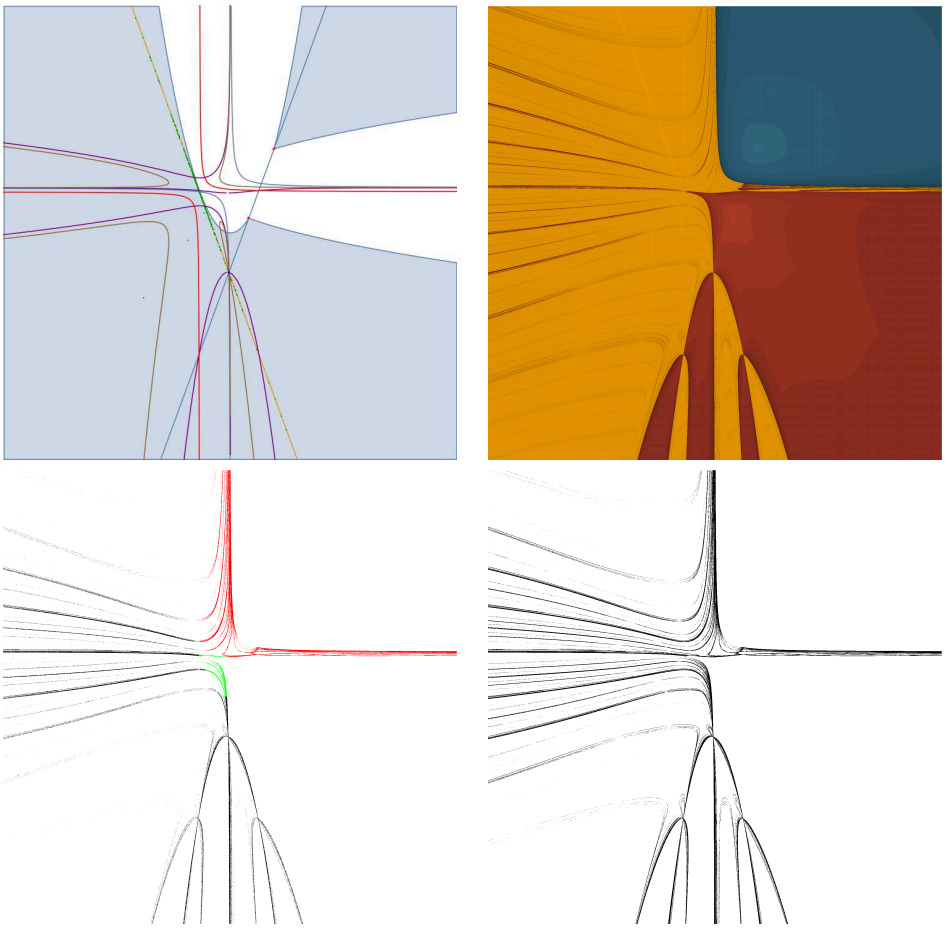

Fig. 6. (Top, left) Main elements in the dynamics of $\mathbf{N}_{-1,2}$: fixed points (red), point of indeterminacy (blue), invariant line joining the two roots and ghost line with its first and second counterimages (purple and gray), the set $\mathbf{Z}_{-1,2}$ (light blue) with its first and second counterimages (red and brown) and first 500 points of the orbit of a random point in the gold region (green). The green points suggest the existence of an attracting chaotic set in the ghost line. (Top, right) Basins of attraction of $\mathbf{N}_{-1,2}$ in the square $[-10, 10]^2$. (Bottom, left) First $3 \cdot 10^5$ points of a random backward orbit of a point below the light blue invariant line under the three branches $w_{1,0}, w_{0,1}, w_{1,1}$ of N_h (in black). Notice that there is a small open set below the line, when the orbit falls there we paint the point in green and choose a different counterimage. The red points are the images of the black points under $w_{0,0}$. (Bottom, right) This picture shows the set $\mathbf{N}_{-1,2}^{-15}(-10, -0.23)$. These two bottom pictures suggest that through α-limits we can only get the set of irregular points of the Julia set.

they are both equal to the set of nonregular points of the boundary of $\mathbf{J}_{-1,2}$.

3.4. *A panorama of maps* $\mathbf{N}_{x_0,y_0}$

In Figs. 7 and 8 we show, respectively, the basins of attraction and a α-limit of the Newton maps of 20 parabolic maps $\mathfrak{f}_{x_0,y_0}$ with $x_0 = -2, -2, 0, 1$ and $y_0 = -2, -1, 0, 1, 2$ to support our Conjectures 1 and 2 under several different situations.

The maps $\mathfrak{f}_{-2,2}$ and $\mathfrak{f}_{-1,1}$ have both four roots and the unions of the four relative basins of attraction of the corresponding Newton maps appear to be full-measure. Similarly, although it has only two roots, it happens for the map $\mathfrak{f}_{0,0}$ already discussed at length in Sec. 3.1. Their α-limits shown in Fig. 8 suggest that regular points of the Julia set are not reached and that these limit sets coincide with the closure of the set of counterimages, under their Newton maps, of the set where these Newton maps have a degenerate Jacobian. Note, though, that each point of the Julia set of the first two Newton maps is a boundary point between basins of attraction corresponding to different roots while, for $x = y = 0$, almost all points of the Julia set have a neighborhood containing the basin of a single root.

For all other maps in Fig. 7 with $y \geq -1$ and $x \leq y$, $\mathfrak{f}_{x,y}$ has only two real roots but three attractors arise: two of them are the basins of attraction of the two real roots while the third one is some

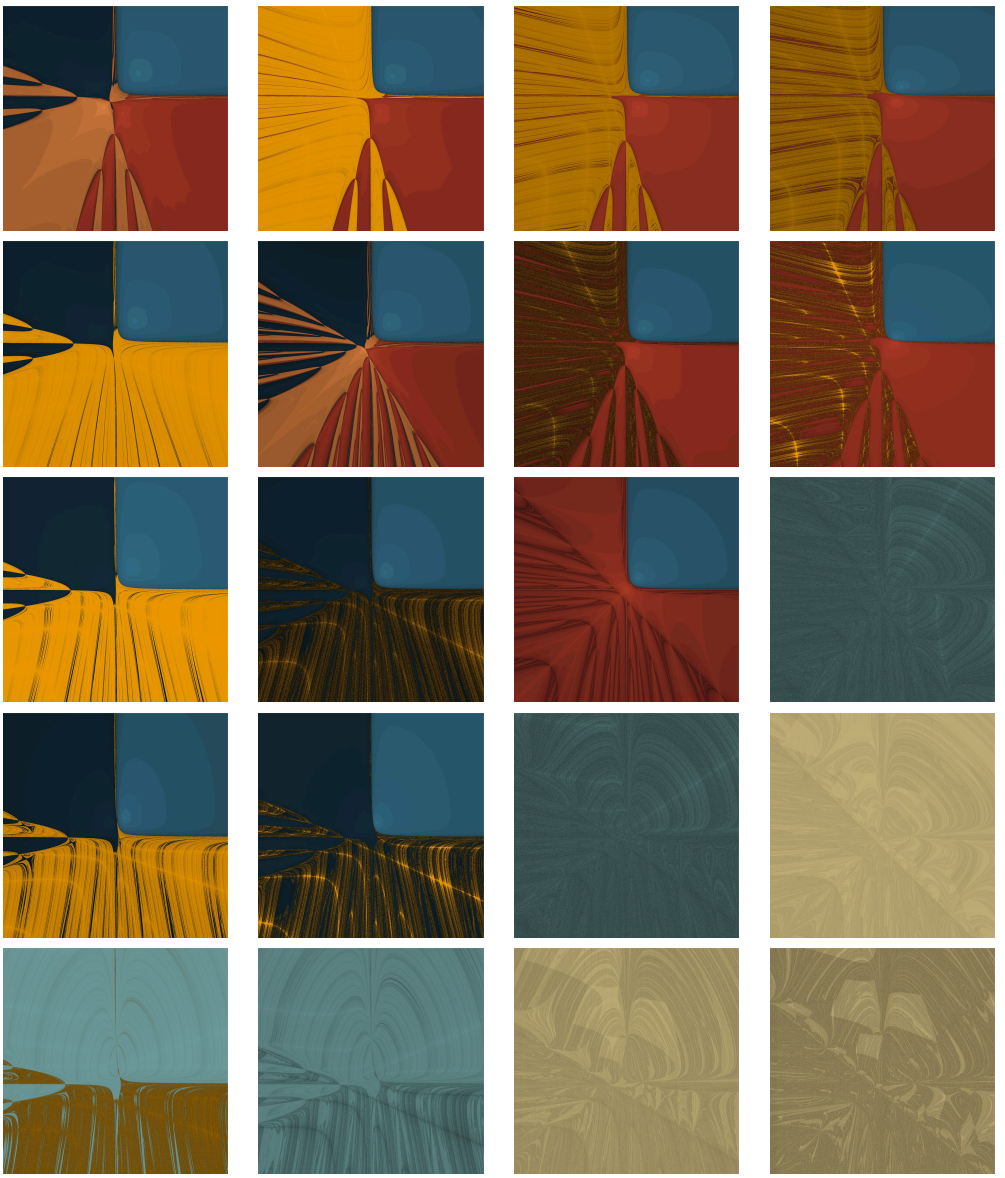

Fig. 7. Basins of attraction for $\mathbf{N}_{x_0,y_0}$ corresponding to the values $x_0 = -2, -1, 0, 1$ and $y_0 = -2, -1, 0, 1, 2$. The numerical results strongly suggest that the union of the basins of attraction of the fixed points corresponding to the roots of $\mathfrak{f}_{x_0,y_0}$ has full Lebesgue measure when the map has four roots and that chaotic attractors, some of which lying on the map's ghost lines, arise when the number of roots of $\mathfrak{f}_{x_0,y_0}$ is not maximal. Darker shades correspond to higher convergence time.

subset on the corresponding ghost line. Numerics suggest that the dynamics on the basin of this third attractor is chaotic, namely it is a subset of the Julia set rather than of the Fatou set like the other two basins. In particular, this means that all corresponding Julia sets have nonempty interior and nonzero measure. The corresponding α-limits shown in Fig. 8 suggest that the interior points of Julia sets cannot be reached.

The remaining maps $\mathfrak{f}_{x,y}$ in Fig. 7 have no real roots and therefore the corresponding Newton maps have two ghost lines. For $x = y = -2$, on each of these two lines lie an attractor, corresponding to the two basins that are visible in the corresponding picture. Note that, in this case, the Julia set is the whole $\mathbb{RP}^2$ since on both basins the dynamics appears to be chaotic. Nevertheless, the corresponding α-limit seems to be the set of boundary points between the two basins. In case of the maps corresponding to pairs (x, y) with $y = x - 1$, only one attractor is visible, the one corresponding to the ghost line associated to the first pair of complex solutions that disappears when y increases. A trace of the α-limit shown in Fig. 8 can be seen also as the

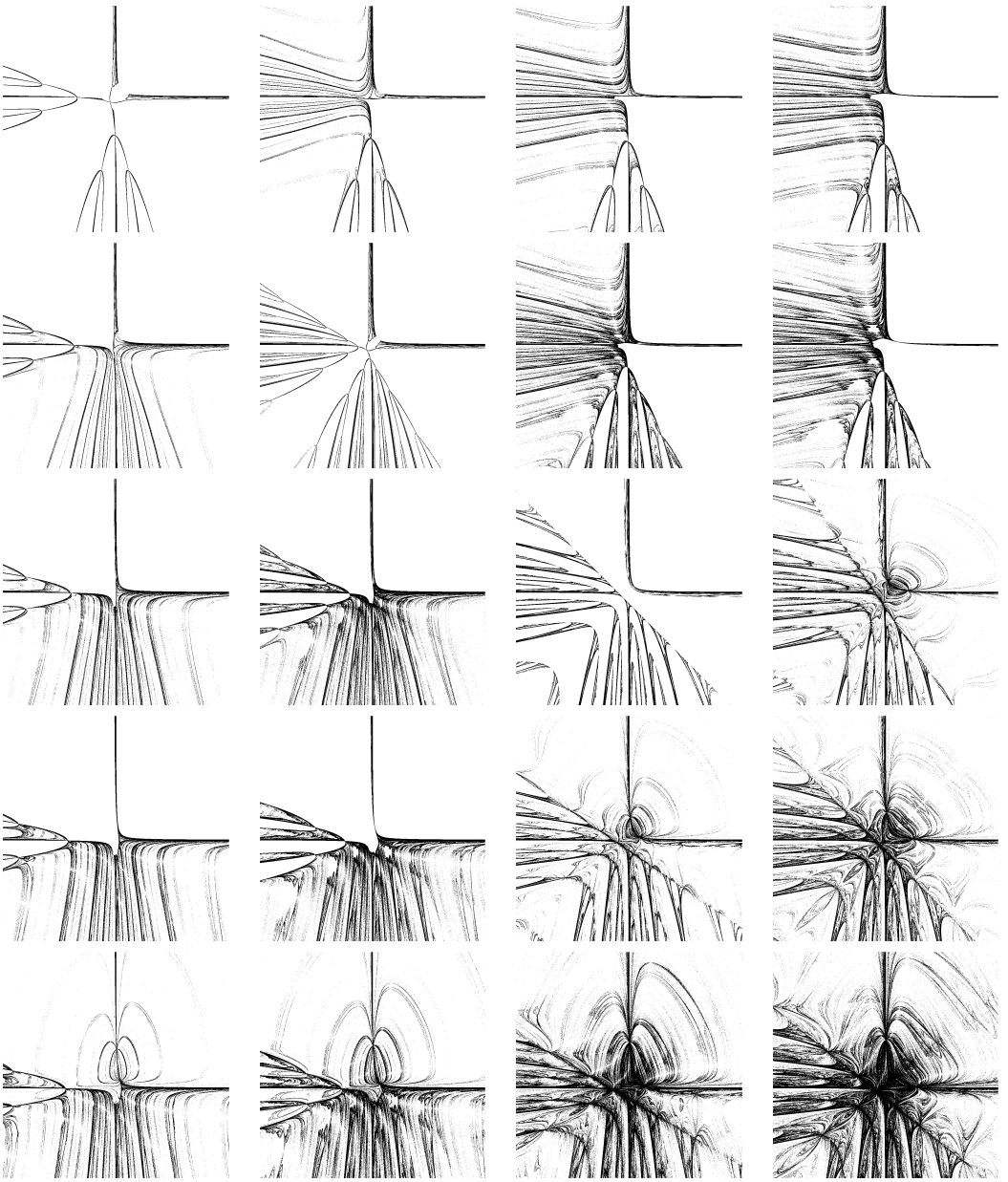

Fig. 8. α-limit of a generic point under the parabolic Newton maps $\mathbf{N}_{x_0,y_0}$ corresponding to the values $x_0 = -2, -1, 0, 1$ and $y_0 = -2, -1, 0, 1, 2$. All these sets are also visible in the previous figure as the nonregular points of the basin boundaries.

darker area, namely the points that converge more slowly, in the picture showing the ω-limits, suggesting again that this α-limit is the closure of the set of the counterimages of the set of degeneracy of the Newton maps Jacobian. Finally, the remaining pictures show, again, a single basin of attraction. This time, though, the attractor is not a subset of either one of the ghost lines — the orbits of generic points seem rather to fill up some two-dimensional region. Just like in the previous case, a trace of the α-limit shown in Fig. 8 can be seen as the darker area in the basin of attraction.

3.5. *The map* $\mathbf{N}_{5,0;1}$

The Newton map

$$\mathbf{N}_{-5,0;1} = \left(\frac{x^3 + xy^2 + 2y - 24x}{2(x^2 + y^2 - 5x)}, \right.$$
$$\left. \frac{y^3 + x^2 y - 10xy + 2x + 24y - 10}{2(x^2 + y^2 - 5x)} \right)$$

has four attractive fixed points $p_1 \simeq (-0.20, -5.1)$, $p_2 \simeq (0.21, 4.7)$, $p_3 \simeq (4.0, 0.25)$ and $p_4 \simeq (6.0, -0.17)$, corresponding to the four roots of $\mathfrak{f}_{5,0;1}$, and restricts to the identity on the circle at infinity.

The four bounded fixed points are super-attractive while the ones at infinity have eigenvalue 1 in the direction of the circle at infinity and a repulsive eigenvalue 2 in some transversal direction depending on the point. The five points of indeterminacy of this map are all bounded: $(0, 0)$, $(5, 0)$ and, approximately, $(4.9, -0.81)$, $(4.7, 1.2)$ and $(0.035, 0.42)$.

Unlike the parabolic case, the map $\mathbf{N}_{-5,0;1}$ is surjective and open, so that its Fatou and Julia sets are fully invariant, as in the complex case. The counterimages of a point (x_0, y_0) are given by

$$w_{\pm}(x_0, y_0) = \left(x_0 \pm \sqrt{\frac{S_+}{2}}, y_0 \mp \sqrt{\frac{S_-}{2}} \right),$$

where

$$S_{\pm} = \sqrt{Q} \pm (24 - 10x_0 + x_0^2 - y_0^2)$$

and

$$Q = 4 + 96x_0^2 - 40x_0^3 - 8x_0y_0 + (-24 + 10x_0 + x_0^2 + y_0^2)^2.$$

Every point has exactly two distinct counterimages except for the fixed points, on which the two counterimages coincide. In Fig. 10 (top, left), we show the fixed (red) and indeterminacy (blue) points, the six invariant lines joining the fixed points, the circle of zeros of the denominator of $\mathbf{N}_{-5,0;1}$ (in blue) and its first counterimage under $\mathbf{N}_{-5,0;1}$ (in purple). The black dots are the 2^{12} points of $N_h^{-12}(-10, -0.23)$ and show how the curves and points drawn fit with the Julia set. Once again the picture suggests that $\mathbf{J}_{-5,0;1}$ is the α-limit of $\mathbf{Z}_{-5,0;1}$.

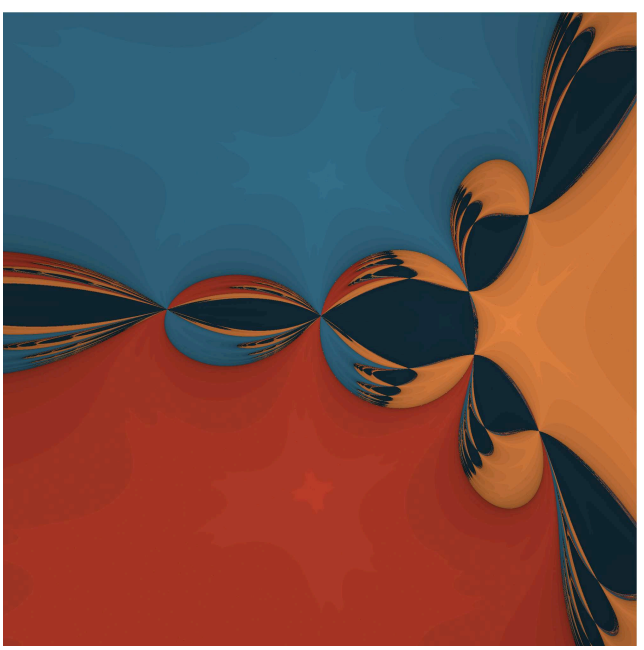

Fig. 9. Basins of attraction of $\mathbf{N}_{5,0;1}$ in the square $[-10, 10]^2$. The four real roots of $\mathfrak{f}_{5,0;1}$ are the points $p_1 \simeq (-0.20, -5.1)$, $p_2 \simeq (0.21, 4.7)$, $p_3 \simeq (4.0, 0.25)$ and $p_4 \simeq (6.0, -0.17)$; the corresponding basins of attraction have been colored, respectively, in red, cyan, blue and mustard. Darker shades correspond to higher convergence time.

Now, let U be a small enough neighborhood of the four fixed points and $X = \mathbb{RP}^2 \backslash U$. Then $\mathbf{N}_{-5,0;1}(X) \supset X$ and so the set $\lim_{n\to\infty} \mathbf{N}_{-5,0;1}^{-n}(X)$ is the compact nonempty repellor of all points that do not leave X under forward iterations of $\mathbf{N}_{-5,0;1}$. Just taking the α-limit of a single point suggests that this limit is the set of irregular points of $\mathbf{J}_{-5,0;1}$ for any nonfixed point of $\mathbf{N}_{-5,0;1}$ [see Fig. 10(bottom right)]. Similarly, $w_{\pm}(X) \subset X$ and so the these two maps define a IFS on X. The numerical evaluation of random orbits under $\mathcal{I}$ [see Fig. 10(bottom, left)] suggests that the irregular points of the Julia set is the unique compact invariant set of $\mathcal{I}$.

3.6. *The map* $\mathbf{N}_{3,-4;1}$

The Newton map

$$\mathbf{N}_{3,-4;1} = \left(\frac{8 + 8x + x^3 + 2y + 8xy + xy^2}{2(-3x + x^2 + 4y + y^2)}, \frac{-6 + 2x - 8y - 6xy + x^2y + y^3}{2(-3x + x^2 + 4y + y^2)} \right)$$

has properties very similar to those of the parabolic map $\mathbf{N}_{-1,2}$.

Like $\mathbf{N}_{-1,2}$, also this map has only two attractive fixed points, namely $p_1 \simeq (7.3, 0.14)$ and $p_2 \simeq (-0.14, -7.0)$, and, correspondingly, only two invariant straight lines and three points of indeterminacy, all bounded: $(0, -4)$, $(3, 0)$ and, approximately, $(2.8, -4.1)$. Like $\mathbf{N}_{5,0;1}$, this map is surjective and open and every point except the fixed one has two counterimages. In Fig. 12 we show all these elements plus the circle $\mathbf{Z}_{3,-4;1}$ and its first counterimage under $\mathbf{N}_{3,-4;1}$.

Just as in case of $\mathbf{N}_{-1,2}$, numerics strongly suggests the presence of a chaotic attractor K lying on the ghost line, whose basin of attraction is shown in gold in Fig. 11. The orbit of a point in $\mathcal{F}(K)$ is shown in green in Fig. 12. Like $\mathbf{N}_{5,0;1}$, both random backward orbits [see Fig. 12(bottom, left)] and the α-limit of a generic point [see Fig. 12(bottom, right)] appear to converge to the set of nonregular points of the Julia set.

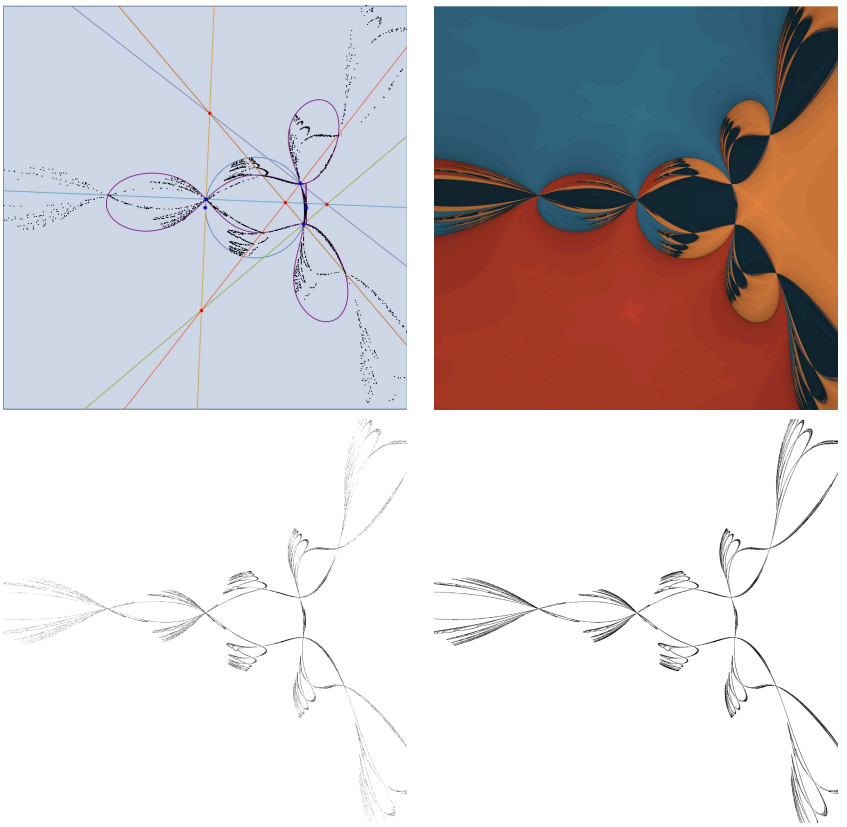

Fig. 10. (Top, left) Some important elements of the dynamics of $\mathbf{N}_{5,0;1}$ in the square $[-10, 10]^2$: fixed points (red), indeterminacy points (blue), the six invariant lines, the set $\mathbf{Z}_{5,0;1}$ (light blue) and its first counterimage (purple). The black points are the counterimages via $\mathbf{N}_{5,0;1}$ of a single point of the plane up to the fifth level of iteration. (Top, right) Basins of $\mathbf{N}_{5,0;1}$ in the square $[-10, 10]^2$. (Bottom, left) First $3 \cdot 10^5$ points of a random backward orbit of a random point under the two branches of $\mathbf{N}_{5,0;1}^{-1}$. (Bottom, right) This picture shows the set $\mathbf{N}_{5,0;1}^{-20}(-10, -3.6)$. These two bottom pictures suggest that through α-limits we can only get the set of irregular points of the Julia set.

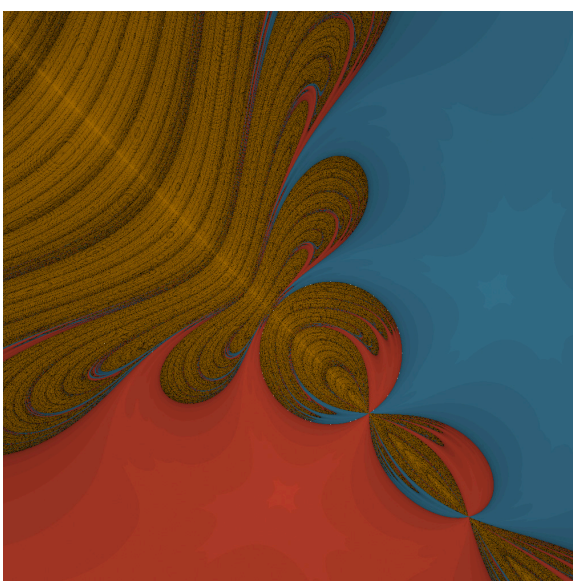

Fig. 11. Basins of attraction of $\mathbf{N}_{3,-4;1}$ in the square $[-10, 10]^2$. The two real roots of $\mathrm{f}_{3,-4;1}$ are the points $p_1 \simeq (7.3, 0.14)$ and $p_2 \simeq (-0.14, -7.0)$, the corresponding basins are colored in cyan and red, respectively. The basin of the third attractor, a chaotic invariant set lying on the ghost line, is colored in gold. Darker shades correspond to higher convergence time. The ghost line is visible in the picture as the set of brightest points of the chaotic attractor.

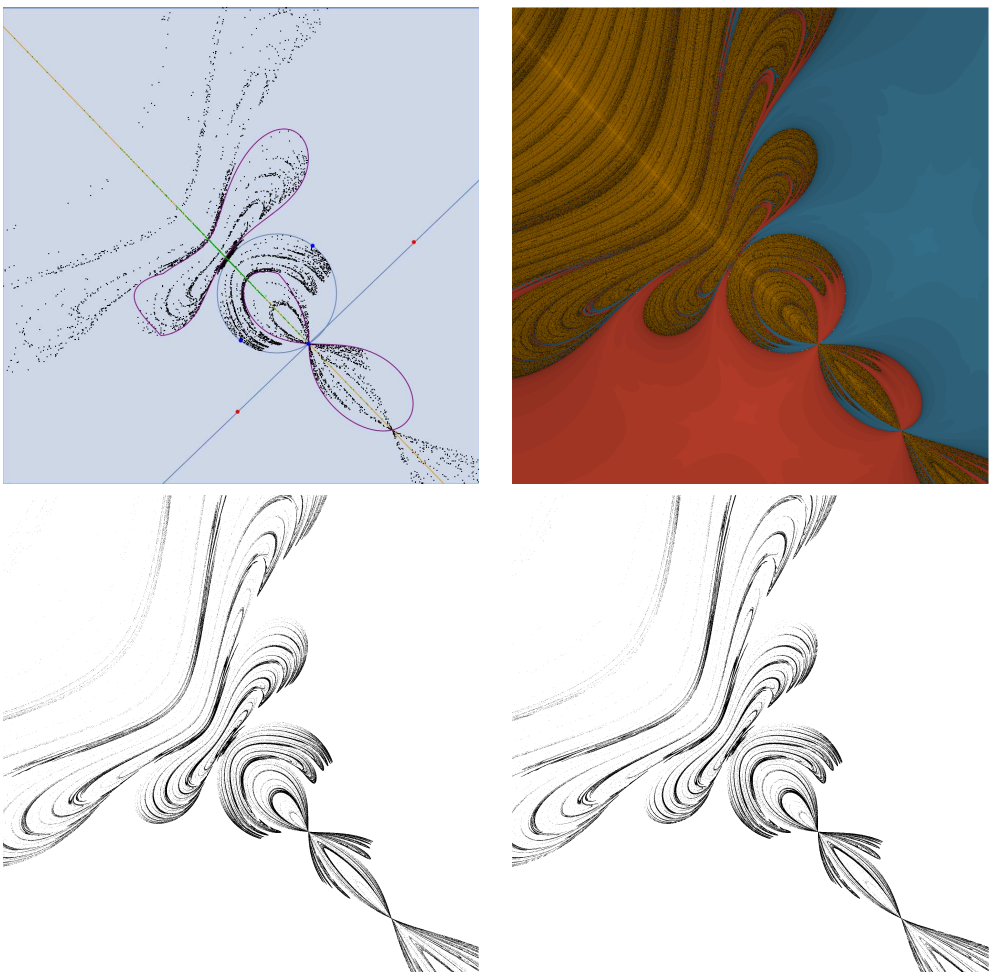

Fig. 12. (Top, left) Main elements in the dynamics of $\mathbf{N}_{3,-4;1}$: fixed points (red), point of indeterminacy (blue), invariant line joining the two roots (light blue) and ghost line (orange), the set $\mathbf{Z}_{3,-4;1}$ (light blue) with its first counterimage (purple). The green and black points are, respectively, the first 500 points of the forward orbit of a random point in the basin of the chaotic attractor and of the backward orbit of a generic point on the plane. (Top, right) Basins of attraction of $\mathbf{N}_{3,-4;1}$ in the square $[-10, 10]^2$. (Bottom, left) First $3 \cdot 10^5$ points of a random backward orbit of a point below the light blue invariant line under the two branches of $\mathbf{N}^{-1}_{3,-4;1}$ (in black). (Bottom, right) This picture shows the set $\mathbf{N}^{-20}_{3,-4;1}(-10, -3.6)$. These two bottom pictures suggest that through α-limits we can only get the set of irregular points of the Julia set.

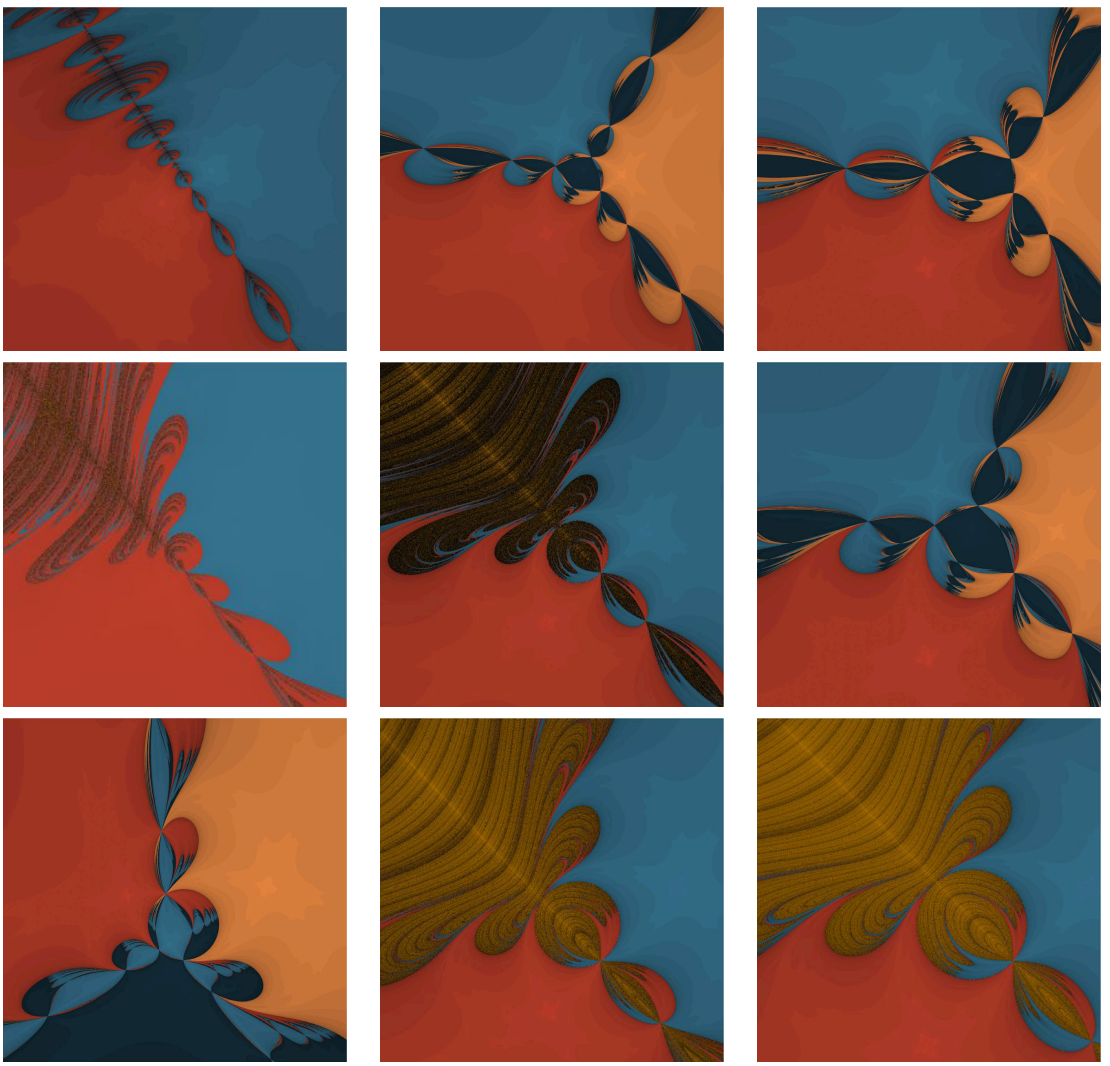

Fig. 13. Basins of attraction, in the square $[-10, 10]^2$, for the hyperbolic Newton maps $\mathbf{N}_{x_0,y_0;1}$ corresponding to the values $x_0 = 1, 3, 5$ and $y_0 = -4, -2, 0$. The numerical results strongly suggest that the union of the basins of attraction of the roots of the corresponding polynomials $\mathfrak{f}_{x_0,y_0;1}$ has full Lebesgue measure when the map has four roots and that a third, chaotic attractor can arise when the number of roots is nonmaximal. Darker shades correspond to higher convergence time.

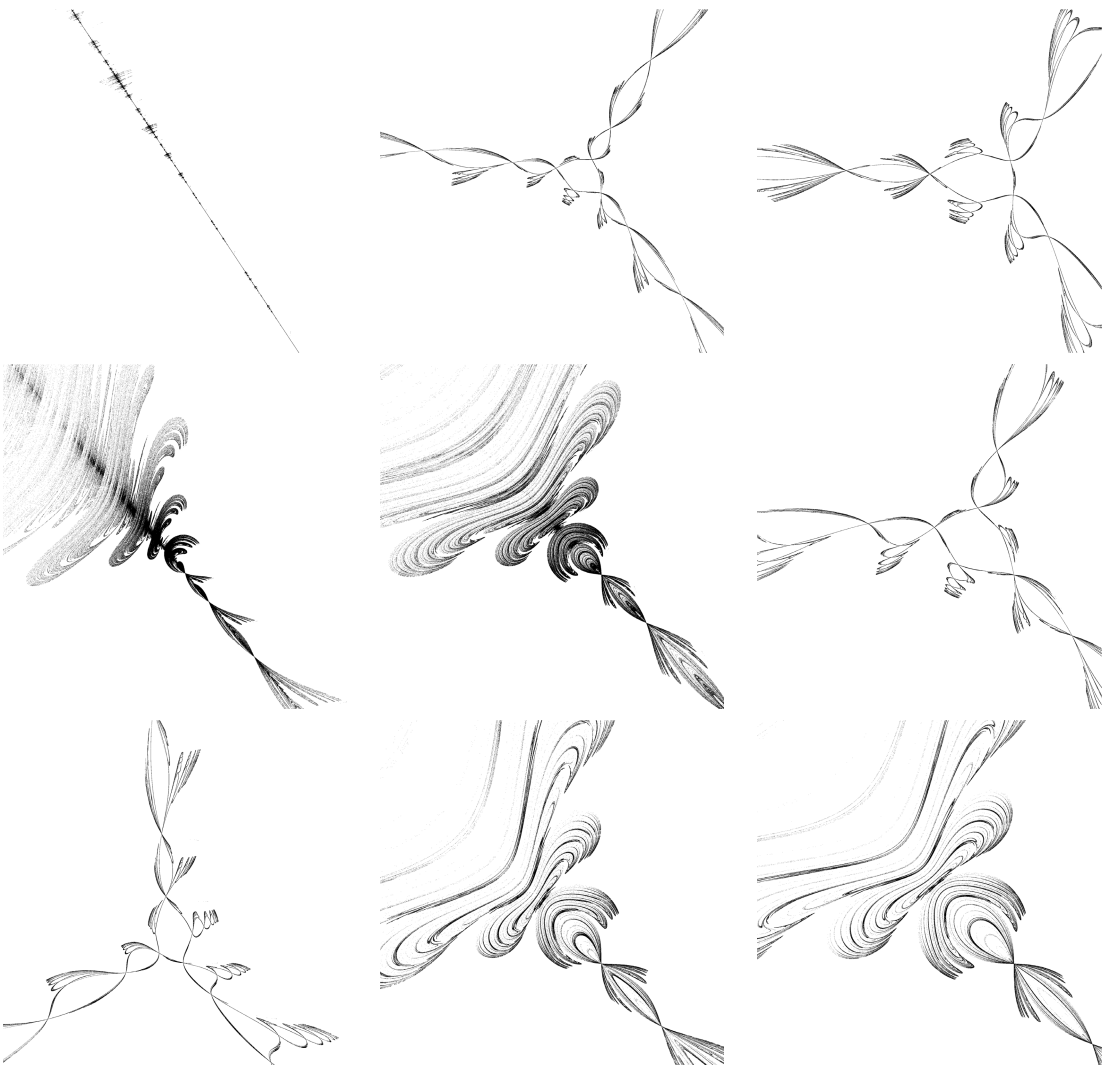

Fig. 14. α-limit of a generic point belonging to some suitable open subset of $\mathbb{RP}^2$ under the parabolic Newton maps $\mathbf{N}_{x_0,y_0;1}$ for the values $x_0 = 1, 3, 5$ and $y_0 = -4, -2, 0$. All these sets are also visible in the previous figure as the nonregular points of the basin boundaries.

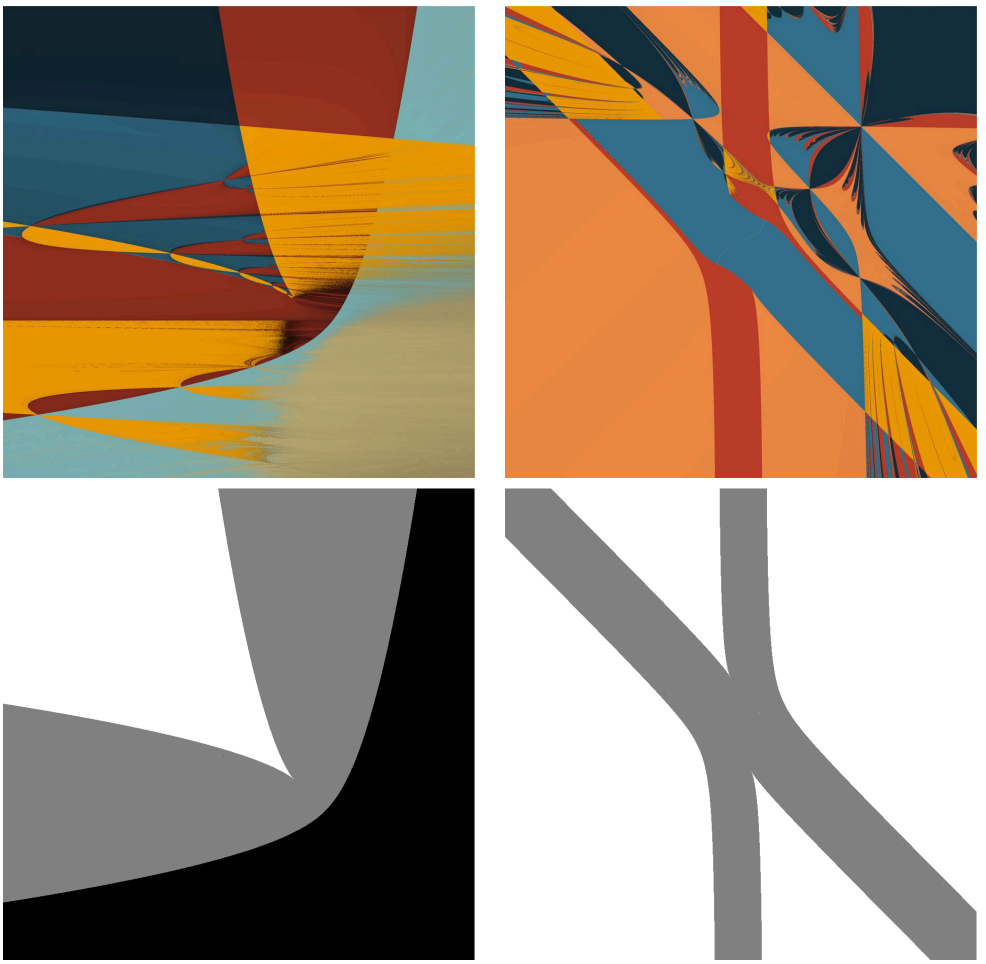

Fig. 15. (Top) Morphology in parameter space for the families of Newton maps $\mathbf{N}_{x_0,y_0}$ and $\mathbf{N}_{x_0,y_0;1}$ in the squares $[-10,5]\times[-5,10]$ and $[-10,10]^2$, respectively. The initial point is $(0,6)$ for the parabolic maps and $(5,5)$ for the hyperbolic ones. (Bottom) Number of solutions in the corresponding squares above: white means four real solutions, gray two real solutions and black no real solution. No attractor besides those of the attracting fixed points were detected in the white regions for the initial points above and several other choices of initial points, supporting Conjecture 2.

3.7. *A panorama of maps* $\mathbf{N}_{x_0,y_0;a}$

In Figs. 13 and 14 we show the basins of attraction and some α-limits of several hyperbolic Newton maps $\mathbf{N}_{x_0,y_0;a}$. Similarly to what we found in the parabolic case, whenever $\mathfrak{f}_{x_0,y_0;a}$ has four roots, the union of the corresponding four basins appear to have full Lebesgue measure in $\mathbb{RP}^2$ while when only two roots appear (a generic map $\mathfrak{f}_{x_0,y_0;a}$ has at least two roots) a third attractor often arises as an invariant subset of the map's ghost line. While the data shown is relative only to the value $a=1$, we could not detect any particular new phenomenon for different values of this parameter. The pictures in Fig. 14 are fully consistent with Conjecture 1 and suggest in a more evident way than their parabolic counterparts that regular points of the Julia set cannot be reached by α-limits.

4. Morphology in Parameter Space

In a celebrated article, Curry *et al.* [1983] found numerical evidence for the existence of cubic holomorphic polynomials of degree 3 whose Newton map has attractive periodic cycles. The theoretical basis of that article is an important general result of Fatou on rational holomorphic maps in one variable: if such a map has an attracting periodic cycle, then one of its critical points must converge to it.

Newton maps of cubic holomorphic polynomials can be parametrized, modulo the equivalence described in Proposition 2, by two real parameters and only one of their critical points is not bound to converge to any of the three bounded attractive fixed points, so checking the ω-limit of this "free" critical point for some large lattice of such maps is enough to detect any "large enough" open subset

of them admitting an attracting cycle. They called the map resulting from this study "Morphology in Parameter Space" (MPS).

In the real case Fatou's result does not hold but analyzing the MPS is anyway interesting for us. For instance, discovering some Newton map of a polynomial with maximal number of real roots having a basin of attraction in addition to those corresponding to those roots would disprove our Conjecture 2. We explored numerically the two-parametric families $\mathbf{N}_{x_0,y_0}$ and $\mathbf{N}_{x_0,y_0;1}$ for several different initial points and found results qualitatively equivalent to those shown in Fig. 15. In both cases, with a striking precision, we detected no extra basin in the region where the corresponding polynomial map has four real roots. Whenever some pattern intersects that region, e.g. like the rocket-shaped pattern in Fig. 15(left), on the intersection the pattern is filled up only with the colors of the basins of attraction of the four roots, giving reason to believe that Conjecture 2 is true for Newton maps of polynomials of type $(2, 2)$. Interestingly enough, notice that the main patterns observable in the basins of the maps $\mathbf{N}_{x_0,y_0}$ and $\mathbf{N}_{x_0,y_0;1}$ appear also in the corresponding MPS.

Acknowledgments

The author gladly thanks J. Yorke for several discussions that greatly helped shaping this article and J. Hawkins for several clarifications. All calculations were performed on the HPCC of the College of Arts and Sciences at Howard University with Python and C++ code by the author. This work was, in part, supported by the National Science Foundation, Grant No. DMS-1832126.

References

Barna, B. [1953] "Über die divergenzpunkte des Newtonschen verfahrens zur bestimmung von Wurzeln algebraischer gleichungen. I," *Publ. Math. Debrecen* **3**, 109–118.

Barnsley, M. [1988] *Fractals Everywhere* (Academic Press).

Barnsley, M. & Demko, S. [1985] "Iterated functions systems and the global construction of fractals," *Proc. Roy. Soc. Lond. A* **399**, 243–275.

Beardon, A. [2000] *Iteration of Rational Functions*: *Complex Analytic Dynamical Systems*, Vol. 132 (Springer Science & Business Media).

Curry, J., Garnett, L. & Sullivan, D. [1983] "On the iteration of a rational function: Computer experiments with Newton's method," *Commun. Math. Phys.* **91**, 267–277.

De Leo, R. [2019] "'Simple dynamics' conjectures for some real Newton maps on the plane," *Fractals* **27**, 1950099.

Fatou, P. [1919] "Sur les équations fonctionnelles," *Bull. Soc. Math. France* **47**, 161–271.

Fatou, P. [1920a] "Sur les équations fonctionnelles," *Bull. Soc. Math. France* **48**, 33–94.

Fatou, P. [1920b] "Sur les équations fonctionnelles," *Bull. Soc. Math. France* **48**, 208–314.

Hubbard, J., Schleicher, D. & Sutherland, S. [2001] "How to find all roots of complex polynomials by Newton's method," *Invent. Math.* **146**, 1–33.

Hubbard, J. & Papadopol, P. [2008] *Newton's Method Applied to Two Quadratic Equations in* $\mathbb{C}^2$ *Viewed as a Global Dynamical System* (American Mathematical Soc.).

Hubbard, J. & Hubbard, B. [2015] *Vector Calculus*, *Linear Algebra*, *and Differential Forms*: *A Unified Approach* (Matrix Editions).

Hurley, M. & Martin, C. [1984] "Newton's algorithm and chaotic dynamical systems," *SIAM J. Math. Anal.* **15**, 238–252.

Hutchinson, J. E. [1981] "Fractals and self-similarity," *Indiana Univ. Math. J.* **30**, 713–747.

Julia, G. [1918] "Memoire sur l'iteration des fonctions rationnelles," *J. Math. Pures Appl.* **1**, 47–246.

Kantorovich, L. [1949] "On Newton's method," *Trudy Mat. Inst. Stek.* **28**, 104–144.

Lagrange, J. [1798] *Traité de la Résolution des Équations Numériques* (Paris).

Lyubich, M. [1986] "The dynamics of rational transforms: The topological picture," *Russ. Math. Surv.* **41**, 43.

Mandelbrot, B. B. [1980] "Fractal aspects of the iteration of $z \to \lambda z(1-z)$ for complex λ and z," *Ann. NY Acad. Sci.* **357**, 249–259.

Miller, J. & Yorke, J. [2000] "Finding all periodic orbits of maps using Newton methods: Sizes of basins," *Physica D* **135**, 195–211.

Milnor, J. [1985] "On the concept of attractor," *The Theory of Chaotic Attractors* (Springer), pp. 243–264.

Milnor, J. [2006] *Dynamics in One Complex Variable*, Vol. 160 (Springer).

Peitgen, H. & Richter, P. [1986] *The Beauty of Fractals*: *Images of Complex Dynamical Systems* (Springer Science & Business Media).

Peitgen, H., Prüfer, M. & Schmitt, K. [1988] "Newton flows for real equations," *Rocky Mountain J. Math.* **18**, 433–444.

Peitgen, H., Prüfer, M. & Schmitt, K. [1989] "Global aspects of the continuous and discrete Newton method: A case study," *Newton's Method and Dynamical Systems* (Springer), pp. 123–202.

Roeder, R. [2005] "Topology for the basins of attraction of Newton's method in two complex variables," Dissertation, Cornell University.

Saari, D. & Urenko, J. [1984] "Newton's method, circle maps, and chaotic motion," *Amer. Math. Month.* **91**, 3–17.

Wong, S. [1984] "Newton's method and symbolic dynamics," *Proc. Amer. Math. Soc.* **91**, 245–253.

Ypma, T. [1995] "Historical development of the Newton–Raphson method," *SIAM Rev.* **37**, 531–551.